Optica Applicata, Vol. XXXIX, No. 4, 2009

An impact of the electrical pumping scheme on some VCSEL performance characteristics

SEWERYN MORAWIEC, PIOTR KOWALCZEWSKI, ROBERT P. SARZAŁA*

Laboratory of Computer Physics, Institute of Physics, Technical University of Łódź,
ul. Wólczańska 219, 90-924 Łódź, Poland

*Corresponding author: rpsarzal@p.lodz.pl

A comprehensive theoretical model of an operation of vertical-cavity surface-emitting diode lasers (VCSELs) is used to compare anticipated room-temperature (RT) continuous-wave (CW) performance of three modern VCSEL designs: the MESA VCSEL with the upper ring contact on the upper *p*-side DBR structure and the bottom broad-area contact as well as the single and the double intra-cavity contacted VCSELs. The MESA VCSEL has been found to demonstrate the best mode selectivity because its desired single fundamental mode operation is expected even for the largest 20-μm diameter devices. However its RT CW lasing thresholds are by about 30% higher than those for both intra-cavity contacted VCSELs because of increasing free-carrier absorption and heat generation. Therefore large-size MESA VCSELs cannot operate at higher temperatures and/or for higher operation currents. On the contrary, although both intra-cavity contacted VCSELs ensure single-fundamental-mode operation for smaller devices only, they seem to operate properly also at higher temperatures and operation currents. Therefore, with an exception of some special applications, intra-cavity contacted VCSELs currently seem to be the best VCSEL designs.

Keywords: vertical-cavity surface-emitting diode lasers (VCSEL), simulation of VCSEL performance.

1. Introduction

Vertical-cavity surface-emitting diode lasers (VCSELs) are distinctly more complex semiconductor devices than previous edge-emitting (EE) diode lasers [1]. But, because of their numerous advantages, VCSELs gradually eliminate EE diode lasers from an increasing number of their applications. The most essential (and unachievable for EE lasers) VCSEL advantages are as follows:

– an inherent single-longitudinal-mode operation even under dynamical conditions,
– a stable low-divergent, circular and without astigmatism output beam,
– a possibility to produce two-dimensional laser arrays, and
– a possibility to monitor both layer thicknesses and compositions during their growth.

Low-divergent VCSEL output beams result from their emission through upper device surfaces. For top-emitting devices, it leads to the annular (ring) upper *p*-side contact with an opening for an output-beam emission. Then current injection into centrally located active region may become non-uniform: it may exhibit the current--crowding effect close to the active-region edge, which may enhance excitation of unwanted higher-order transverse modes. Currently there are three the most promising modern VCSEL structures shown in Fig. 1:

– the MESA VCSEL (Fig. 1**a**) with the upper ring contact on the upper *p*-side DBR structure and the bottom broad-area contact,

– the single intra-cavity-contacted (SI) VCSEL (Fig. 1**b**) with the upper ring contact on the upper *p*-type spacer and the bottom broad-area contact,

– the double intra-cavity-contacted (DI) VCSEL (Fig. 1**c**) with ring contacts on both the *n*-type and *p*-type spacers.

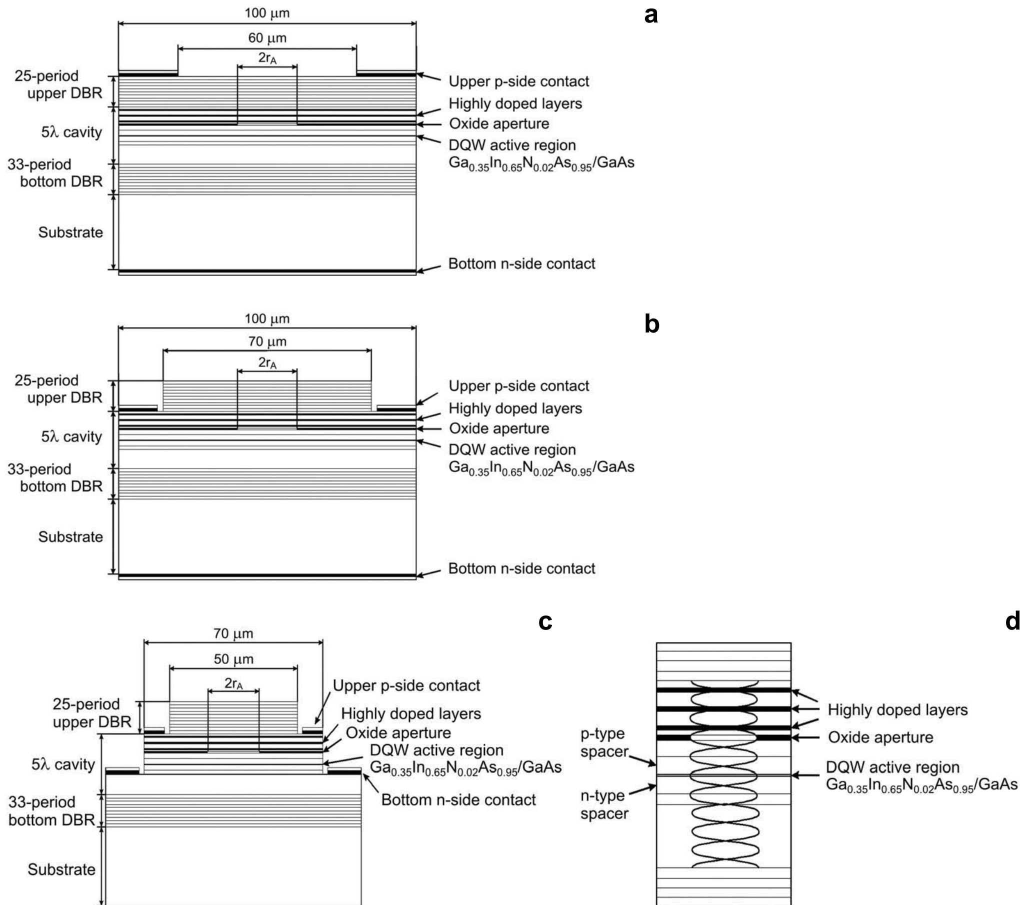

Fig. 1. Three the most promising VCSEL structures: the MESA VCSEL (**a**), the single intra-cavity--contacted VCSEL (**b**), the double intra-cavity-contacted VCSEL (**c**). A structure of the 5λ cavity (**d**).

The MESA and the DI VCSEL designs have been manufactured and compared in Nanophotonics Center, Industrial Technology Research Institute, Hsinchu (Taiwan), Department of Electrophysics, National Chiao Tung University, Hsinchu (Taiwan), Institute of Microelectronics, National Cheng Kung University, Tainan (Taiwan) and A. F. Ioffe Physical-Technical Institute, St. Petersburg (Russia) [2]. In the MESA VCSEL, the current spreading from the upper ring contact towards the centrally located active region takes place through the upper *p*-side DBR mirror. Therefore this DBR structure should be doped, which increases an unwanted free-carrier absorption and the VCSEL lasing threshold. Nevertheless, current injection into active region of the MESA VCSEL is nearly perfectly uniform, which enhances excitation of the desired single fundamental LP_{01} mode. In both intra-cavity-contacted VCSELs, their current paths omit the upper *p*-side DBR mirrors, therefore they may be intentionally undoped, which reduces absorption. But, on the other hand, the upper radial current-spreading layer may be too thin to ensure the above uniform current injection into VCSEL active regions, which may enhance an excitation of higher-order transverse modes and which reduces the VCSEL mode selectivity. Therefore the main goal of this work is to compare, with the aid of the comprehensive fully self-consistent VCSEL model, anticipated performance characteristics of all three the above VCSEL designs to choose the best VCSEL configuration for its current applications.

2. Model

Following principles given by NAKWASKI [3], the comprehensive optical-electrical--thermal-gain self-consistent VCSEL threshold model has been developed to simulate a room-temperature (RT) continuous-wave (CW) operation of the diode laser under consideration. The model consists of four mutually interrelated parts:

– the three-dimensional (3D) optical model (the effective-frequency method proposed by WENZEL and WÜNSCHE [4]) describing, for successive radiation modes, their modal gain and losses, lasing thresholds, emission wavelengths and optical field distributions within the laser cavity,

– the 3D finite-element-method (FEM) electrical model characterizing the current spreading between the top and the bottom annular contacts through the centrally located active region, the injection of carriers of both kinds into the QW active region and their subsequent radiative or non-radiative recombination after radial 2D out-diffusion within the active layer,

– the 3D FEM thermal model characterizing generation of the heat flux (non--radiative recombination, reabsorption of spontaneous radiation as well as volume and barrier Joule heating), its flow from the heat sources towards the heat sink and its spreading within the heat-sink, and

– the gain model (the Fermi's Golden Rule) furnishing information about an optical gain process within the QW active region to enable determination of its optical-gain spectra.

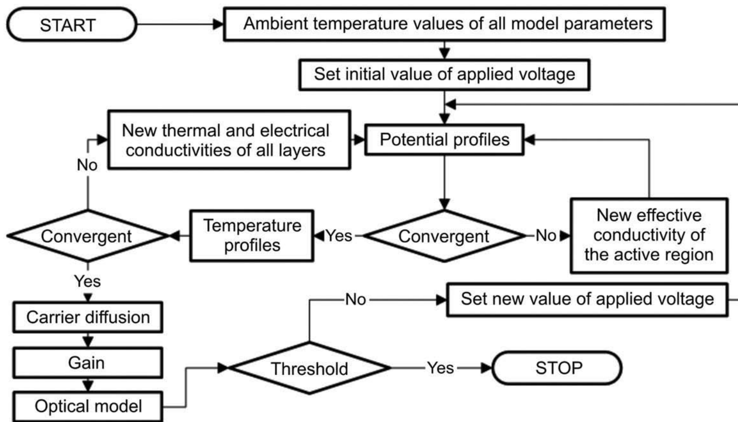

Fig. 2. A flow chart of the iteration algorithm used in our self-consistent threshold VCSEL simulation.

In this theoretical approach, all important, usually non-linear, interactions between optical, electrical, thermal and recombination phenomena are taken into account with the aid of the self-consistent approach (Fig. 2). Accordingly, in each loop of the self-consistent calculation algorithm, new 3D profiles of all model parameters within the whole device volume are determined not only on the basis of various chemical compositions of its structure layers but also taking into account current 3D profiles of the temperature, the current density, the carrier concentration and the mode radiation intensity. Therefore we consider our model as a fully self-consistent one. More details of the model have been reported by SARZAŁA and NAKWASKI [5] and SARZAŁA [6]. Validity of our model has been confirmed experimentally [7].

3. Structure

The present analysis has been carried out assuming, for all three VCSEL designs (Fig. 1) under consideration, the same modern GaAs-based oxide-confined double-quantum-well (DQW) GaInNAs/GaAs VCSEL configuration [8] emitting the 1.3-μm radiation. The active region consists of two (GaIn)(NAs) quantum wells of thicknesses equal to 11 GaAs lattice constants (11·0.5653 nm = 6.2183 nm), each containing 35% indium and 2% nitrogen, separated by the 11.3-nm GaAs barrier and sandwiched by the GaAs spacers, all intentionally undoped (residual 10^{15} cm^{-3} doping is assumed). The active region is surrounded by the *p*-type and the *n*-type GaAs spacers. Relatively high doping ($4 \cdot 10^{18}$ cm^{-3}) of the areas close to the successive node positions of the standing optical wave within the *p*-type contact layer (Fig. 1**d**) is applied to reduce their electrical resistivities because they are also working as the radial-current-spreading layers for a current flow from the upper annular contacts towards the central active region. The highly-doped (10^{18} cm^{-3}) 55.0-nm $Al_{0.98}Ga_{0.02}As$ layer is manufactured at the analogous anti-node position within the upper *p*-type contact layer close to the active region. This layer is used to create within it the proper Al_xO_y

oxide aperture introducing radial confinements for both the current spreading and the electromagnetic field. The *n*-type spacer and the remaining parts of the *p*-type spacer are doped only to $1\cdot10^{17}$ cm^{-3} to reduce the free-carrier absorption. The upper and bottom distributed Bragg reflectors (DBRs) consisting, respectively, of 25 and 33 periods of the quarter-wave $GaAs/Al_{0.9}Ga_{0.1}As$ layers are manufactured as DBR mirrors of the 5λ laser cavity. As the *n*-side and the *p*-side contacts, the AuGe/Ni/Au and Ti/Pt/Au, respectively, contacts are deposited. The laser is stuck on the copper heatsink with the aid of the 5-μm indium solder. All three VCSEL designs have 100-μm diameters. For the MESA VCSEL, the internal contact diameter is equal to 60 μm. The upper *p*-side DBR mirror of the 70 μm diameter has been produced in the SI VCSEL. In the case of the DI VCSEL, analogous 50-μm diameter upper *p*-side DBR mirror has been manufactured, whereas the main VCSEL part between both the contacts has a diameter of 70 μm.

4. Results

Figure 3 presents plots of maximal values of the RT CW threshold optical gain g_{th} versus the radius r_A of active regions of DI and MESA VCSELs. Both plots are very similar to each other: for very small active regions, lasing threshold is rapidly

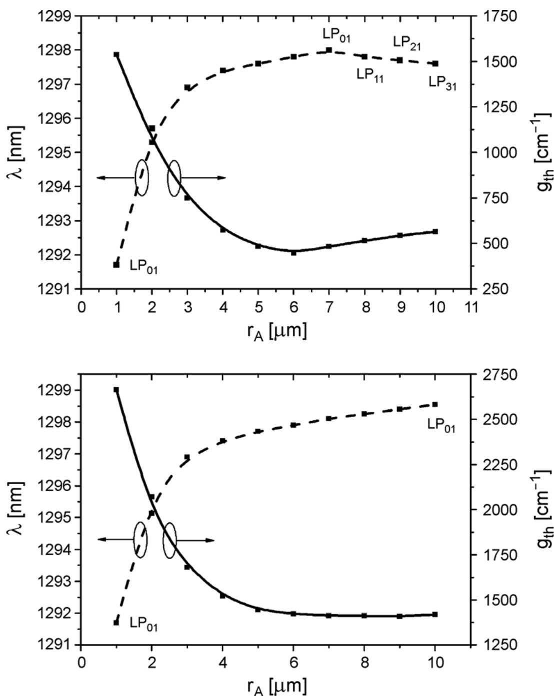

Fig. 3. Maximal value of the RT CW threshold active-region gain g_{th} and wavelength λ of emitted radiation versus the radius r_A of the VCSEL active region determined for: the DI VCSEL (**a**), and the MESA VCSEL (**b**). The lowest-threshold transverse LP modes are indicated.

decreased with an increase in r_A because of a steady improvement of radial confinement of the radiation field whereas, for larger active regions, this decrease is reduced to zero (MESA VCSEL) or even the lasing threshold is somewhat increased (DI VCSEL). The indicated different behaviour of both VCSEL designs is a result of an excitation of higher-order transverse LP modes in larger DI VCSELs, while, in MESA ones, a stable single-fundamental-mode operation is preserved for the whole range of active-region sizes.

The above important advantage of MESA VCSELs follows from their almost perfectly uniform current injection into even very large active regions (Fig. 4), which is favourable for the fundamental LP_{01} transverse mode. In both SI and DI VCSELs, on the other hand, a distinct current crowding effect is seen in the area close to the active-region edge, which enhances an excitation of higher-order transverse modes of somewhat higher optical losses. The SI VCSELs exhibit a little higher threshold currents than DI ones because of their current flow through the bottom n-side DBR mirror. A steady increase in the wavelength λ of MESA VCSELs with an increase in the active-region size follows from a steadily reduced penetration by its radiation field of the oxide aperture of a very low index of refraction. Analogous λ decrease observed in large-size DI VCSELs is caused by increasing penetration of this area by higher-order transverse modes.

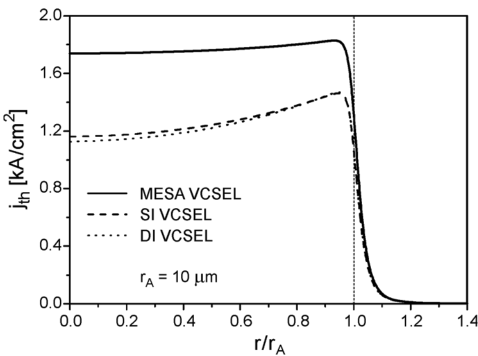

Fig. 4. Radial profiles of the RT CW threshold current densities j_{th} of three considered VCSEL designs (MESA, SI and DI VCSELs) for their active-region radii r_A of 10 μm.

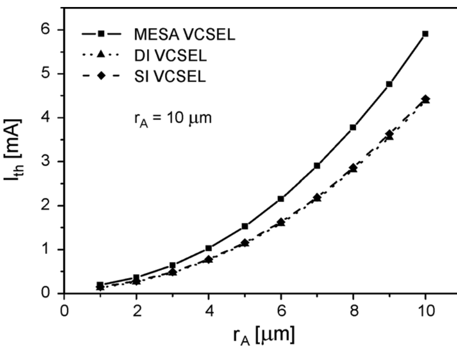

Fig. 5. RT CW threshold current I_{th} of three considered VCSEL designs (MESA, SI and DI VCSELs) versus radii r_A of their active regions.

The MESA VCSEL exhibits much better mode selectivity than both SI and DI ones, but its lasing threshold is definitely much higher, which is already seen in Fig. 4 and which may be also seen in Fig. 5, presenting RT CW threshold currents I_{th} of VCSELs under consideration versus radii of their active regions. This behaviour results from the free-carrier absorption within the upper DBR mirrors of the MESA VCSELs and from an additional heat generation within those mirrors resulting in their active-region temperatures about 30% higher than those of the SI and DI VCSELs.

Uniformity of current injection into active regions of intra-cavity contacted VCSELs may be considerably improved with an increase in p doping of layers located at successive node positions of the standing optical wave within the p-type spacers (Fig. 1**d**). It is clearly seen in Fig. 6, presenting, for the DI VCSEL with the 10-μm active-region radius, radial profiles of the injected threshold current density j_{th}. As one

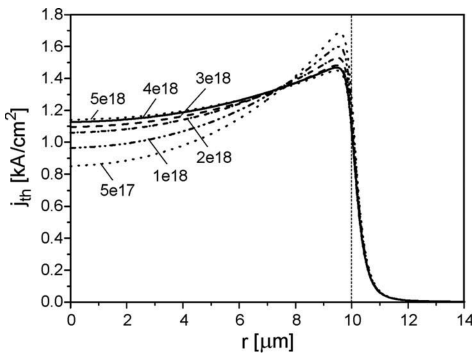

Fig. 6. Radial plots of the RT CW threshold current density j_{th} of the DI VCSEL within the active-region of 10-μm radius for an increasing doping of the highly-doped layers at successive node positions of the standing optical wave within the p-type spacer.

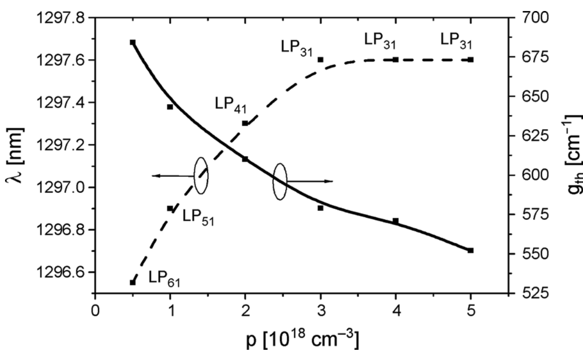

Fig. 7. Maximal value of the RT CW threshold active-region gain g_{th} and the wavelength λ of emitted radiation of the DI VCSEL with the active-region radius of 10 μm versus doping p of the highly-doped layers at successive node positions within the p-type spacer. The lowest-threshold LP modes are indicated.

can see, an improvement in the current uniformity is very distinct for relatively low doping, but its impact becomes nearly negligible for $p > 3\cdot10^{18}$ cm^{-3}. As a result, in Fig. 7, maximal values of the threshold optical gain $g_{\rm th}$ are seen to be steadily reduced for increasing p up to its $3\cdot10^{18}$ cm^{-3} value. At the same time, lower-order transverse modes become the lowest-threshold ones, but this process has been finished for the $\rm LP_{31}$ mode.

5. Conclusions

Room-temperature (RT) continuous-wave (CW) performance of three various VCSEL designs, *i.e.*, the MESA VCSEL, the single (SI) and the double (DI) intra-cavity contacted VCSELs, have been analysed and compared with the aid of our comprehensive fully self-consistent VCSEL model. The MESA VCSEL has been found to demonstrate the best mode selectivity, which means – a desired single fundamental mode operation for all the considered active-region sizes. It is a result of its nearly perfectly uniform current injection into active regions. But, on the other hand, its RT CW threshold current is by nearly 30% higher than threshold currents of both SI and DI VCSELs, which follows from an increased free-carrier absorption in its DBR mirrors and an increased heat generation within those mirrors. Therefore, the above single fundamental mode operation does not seem to be stable, the MESA VCSEL is expected to stop lasing completely at higher temperatures and/or for higher operation currents.

Both intra-cavity contacted VCSELs of larger active regions suffer from excitation of higher-order transverse modes because of increasingly non-uniform current injection into their active regions. This effect limits their single-fundamental-mode operation to not too high output powers. The above uniformity of current injection may be improved a little with the aid of higher doping of areas close to successive node positions of the optical standing wave within the p-type spacer. Anyway, intra-cavity contacted VCSELs seem to offer much better RT CW performance than the MESA VCSELs, also because of their much lower RC time constants which are necessary for a high-speed modulation.

Acknowledgements – The authors would like to acknowledge the support from the Polish Ministry of Science and Higher Education (MNiSzW), grant No. N N 515 417635.

References

[1] MROZIEWICZ B., BUGAJSKI M., NAKWASKI W., *Physics of Semiconductor Lasers*, North-Holland, Amsterdam 1991, Chapter 4.

[2] YANG H.-P.D., LU C., HSIAO R., CHIOU C., LEE C., HUANG C., YU H., WANG C., LIN K., MALEEV N.A., KOVSH A.R., SUNG C., LAI C., WANG J., CHEN J., LEE T., CHI J.Y., *Characteristics of MOCVD- and MBE-grown InGa(N)As VCSELs*, Semiconductor Science and Technology **20**(8), 2005, pp. 834–839.

[3] NAKWASKI W., *Principles of VCSEL designing*, Opto-Electronics Review **16**(1), 2008, pp. 18–26.

[4] WENZEL H., WÜNSCHE H.-J., *The effective frequency method in the analysis of vertical-cavity surface-emitting lasers*, IEEE Journal of Quantum Electronics **33**(7), 1997, pp. 1156−1162.
[5] SARZAŁA R.P., NAKWASKI W., *Optimization of 1.3 μm GaAs-based oxide-confined (GaIn)(NAs) vertical-cavity surface-emitting lasers for low-threshold room-temperature operations*, Journal of Physics: Condensed Matter **16**(31), 2004, pp. S3121−S3140.
[6] SARZAŁA R.P., *Designing strategy to enhance mode selectivity of higher-output oxide-confined vertical-cavity surface-emitting lasers*, Applied Physics A: Materials Science and Processing **81**(2), 2005, pp. 275−283.
[7] XU D., TONG C., YOON S.F., FAN W.-J., ZHANG D.H., WASIAK M., PISKORSKI Ł., GUTOWSKI K., SARZAŁA R.P., NAKWASKI W., *Room-temperature continuous-wave operation of the In(Ga)As/GaAs quantum-dot VCSELs for the 1.3 μm optical-fibre communications*, Semiconductor Science and Technology **24**(5), 2009, p. 055003.
[8] RAMAKRISHNAN A., STEINLE G., SUPPER D., STOLZ W., EBBINGHAUS G., *Nitrogen incorporation in (GaIn)(NAs) for 1.3 μm VCSEL grown with MOVPE*, Journal of Crystal Growth **248**, 2003, pp. 457−462.

Received June 19, 2009